Available online at www.sciencedirect.com

ScienceDirect

Energy Procedia 69 (2015) 1160 – 1170

Energy Procedia

International Conference on Concentrating Solar Power and Chemical Energy Systems
SolarPACES 2014

A high-efficiency solar thermal power plant using a dense particle suspension as the heat transfer fluid

J. Spelling[a,*], A. Gallo[a], M. Romero[a], J. González-Aguilar[a]

[a] *High Temperature Processes Unit, IMDEA Energy Institute, 28935 Móstoles, Spain*

Abstract

A novel solar power plant concept is presented, based on the use of a dense particle suspension as the heat transfer fluid which allows receiver operation at high temperatures (above 650°C), opening the possibility of using high-efficiency power generation cycles such as supercritical Rankine cycles. A 50 MW_e solar power plant was designed based on this new heat transfer fluid and compared with a conventional molten salt solar power plant. The supercritical Rankine-cycle power block increases the thermal conversion efficiency from 39.9% to 45.4%, corresponding to a 9.6% reduction in the size of the heliostat field. The operating temperature range is increased by 24.5%, which leads to a 12.5% increase in storage density and a 22.5% reduction in the total storage volume. Parasitic power consumption is also reduced due to the elimination of the need for heat tracing. Overall, the combination of increased cycle efficiency, increased storage density and reduced parasitics to leads to a predicted electricity cost reduction of 10.8%.

Peer review by the scientific conference committee of SolarPACES 2014 under responsibility of PSE AG

Keywords: dense particle suspension; supercritical steam-cycle; high efficiency solar power

1. Introduction

Concentrating solar power (CSP) is almost unique amongst renewable energy technologies in that it can supply controllable power on demand to consumers [1]. Through the integration of thermal energy storage, excess solar

* Corresponding author. Tel.: +34-91-737-1150; fax: +34-91-737-1140.
E-mail address: james.spelling@imdea.org

Peer review by the scientific conference committee of SolarPACES 2014 under responsibility of PSE AG
doi:10.1016/j.egypro.2015.03.191

energy can be stored during daytime and used to extend power generation during cloud passages or at night. The dispatchable nature of CSP plants makes them ideally suited to form the backbone of a future low-carbon electricity grid, providing reliable generation capacity to support other renewable technologies.

However, despite these promising attributes, electricity from CSP plants remains more expensive than from solar photovoltaics and wind. As dispatchability is not currently valued by the majority of incentive schemes [2], CSP plants cannot exploit their unique characteristics and deployment has slowed in recent years. A step change in CSP technology is required in order to drive down costs and ensure competitiveness in a liberalized electricity market.

Central to the challenges faced by CSP is the fact that over 80% of all installed capacity is still based on parabolic trough technology [3], developed nearly 30 years ago. Parabolic trough CSP plants employ Rankine-cycle power blocks with low temperature (< 400ºC) steam turbines, which operate with relatively low efficiencies (~35% when dry-cooled [3]). Reaching higher temperatures is seen as key to future cost reductions, as higher temperatures lead to both higher power conversion efficiencies and increased storage densities. As such, higher operating temperatures can directly reduce the total cost of the solar collector field and the specific cost of the storage units. With solar field costs accounting for up to 50% of the total cost of the power plant [1], significant reductions in the overall cost of electricity can be expected.

In recent years, two competing technologies have emerged to achieve higher temperatures, namely molten-salt and direct steam generation towers [4], which have successfully demonstrated higher efficiencies and lower costs. Despite this, both technologies have their associated drawbacks. Molten-salt systems are limited to operating temperatures below 550°C by the thermal stability of the salt itself, preventing the use of even more efficient, higher temperature power conversion cycles. Molten-salt systems also suffer from freezing problems if the salt temperature drops too low, resulting in a high parasitic power consumption for heat-tracing. Direct steam systems are not limited in the temperatures they can achieve, as no intermediary heat transfer fluid is used. However, they typically operate with steam temperatures in the region of 565°C and no large-scale storage system has been developed for live steam. Use of this technology therefore negates a key advantage of CSP: the ability to store energy [4].

As such, if the true potential of CSP technology is to be harnessed, new heat transfer fluids (HTFs) are needed that can both reach higher temperatures and easily be stored. This paper addresses the design of a high-efficiency solar thermal power plant using one such HTF: the dense gas-particle suspension.

2. The dense particle suspension as a novel heat transfer fluid

The dense particle suspension (DPS) is an alternative to the classical HTFs used in CSP plants, combining the good heat transfer properties of liquids and the ease of handling of gases with the high temperature properties of solid particles. The DPS consists of very small particles which can be fluidized at low gas speeds (group A of Geldart's classification [5]); these fluidized particles can then be easily transported in a similar manner to a gas. The fraction of particles within the fluidized suspension is high (up to around 40% by volume [6]), resulting in a fluid with a high density (above 1000 kg/m^3 [6]), similar to that of a liquid, and a significant improvement in heat transfer compared to the entraining gas alone (heat transfer coefficients in the range of 500 to 750 W/m^2K [7]). If ceramic particles are considered, the DPS can be used at extremely high temperatures (up to 1000°C [8]), limited only by the material of the absorber tubes. Ceramic particles are chemically inert and present no risk of explosion. Furthermore, due to the high particle density, and the ease of separating the particles from the entraining gas flow, energy storage can be easily implemented through simple bulk storage of hot particles. As the particles are solid, they cannot freeze, removing the lower temperature limit and heat tracing problems associated with molten salts.

By allowing an increase in the operating temperature of the receiver, the use of a DPS as a new HTF in CSP plants causes a cascade of effects, which are summarized in Fig. 1. Higher temperature operation has two immediate effects: firstly an increase in the power cycle efficiency and secondly an increase in the temperature range over which the storage tanks operate, which increases the storage density. The increased efficiency of the power cycle also reduces the thermal power demand, which allows a smaller heliostat field to be used and more electricity to be generated from each unit of stored thermal energy. The smaller heliostat field is both cheaper and more efficient, and the increased capacity of the storage allows the power plant capacity factor to be increased.

While an increase in cycle efficiency is guaranteed to reduce the cost of the heliostat field, the effects on the other components of the CSP plant are more difficult to predict. Higher temeprature operation will almost certainly

increase the cost of the receiver and possibility the power cycle as well (depending on the choice of technology). The increase in storage density and capacity acts to drive down costs, however higher temperature operation will also potentially require the use of more expensive construction materials. As such, if the new high-temperature HTF is to improve the economics of CSP, the cost reductions for the solar field and storage must more than outweight any increases in the cost of the receiver and power cycle.

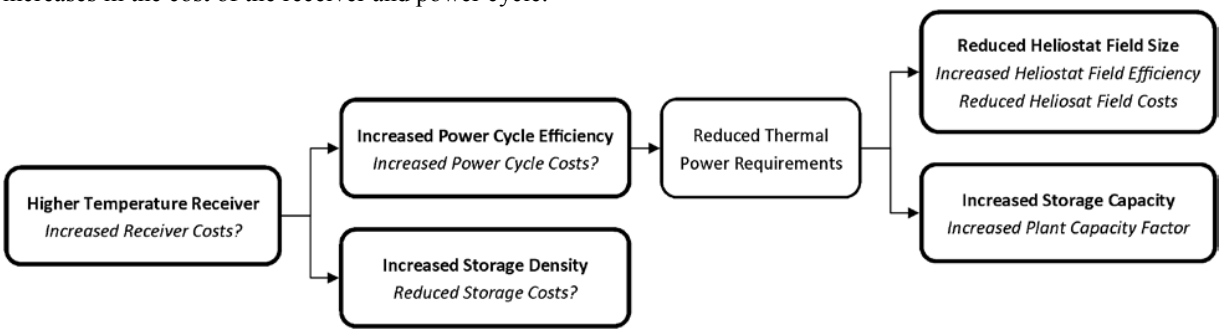

Fig. 1. Effects of an increase in receiver temperature.

3. High-efficiency solar thermal power plants using the dense particle suspension

In order to quantify and evaluate both the technical and economic potential of the DPS, this paper presents the design of a 50 MW_e CSP plant based around this new HTF and compares it with the performance of an identically sized conventional molten salt power plant. The layout of the new power plant is shown schematically in Fig. 2. Five core power plant components can be identified, namely the heliostat field, the particle receiver, the thermal energy storage system, the heat exchanger network and the power block. Transport of the solid particles from the storage to the receiver must also be considered, as well as particle transport within the heat exchangers.

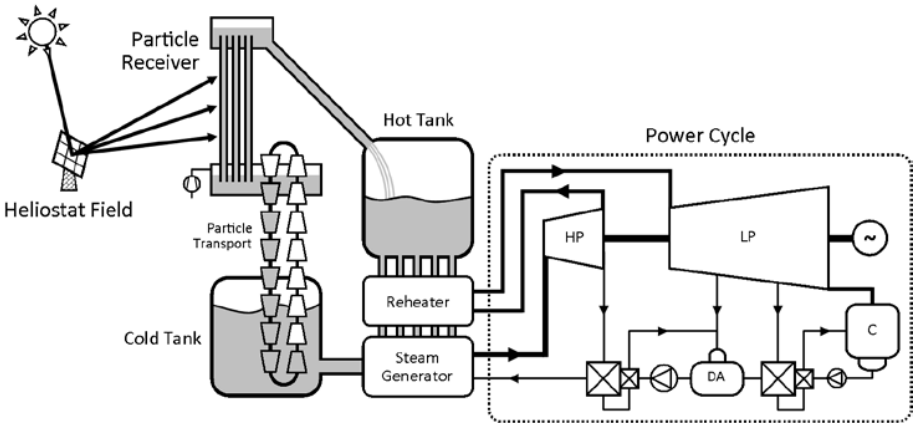

Fig. 2. Schematic layout of a dense gas-particle suspension power plant.

In order to ensure that an objective comparison is made between the DPS and molten salt CSP plants, a standard set of power plant specifications has been established; the chosen values are shown in Table 1. The higher operating temperature of the DPS allows advanced Rankine cycle power block configurations to be used, the full potential of which are not exploited in contemporary CSP plants.

A set of the most common Rankine cycle configurations [11] [12] are shown in Fig. 3, in terms of the live steam temperatures and pressures, along with typical efficiency values; additional information concerning the configurations is presented in Table 2. Parabolic trough CSP plants are limited to steam temperatures below 385°C by their thermal oil HTF; similarly molten salt CSP plants are limited to temperatures below 550°C [4]. It can be

clearly seen that state-of-the-art parabolic trough and molten salt power plants (configurations 1 and 2) operate at temperatures and pressures far below the corresponding state-of-the-art fossil plants, resulting in lower efficiencies.

Table 1. Power plant design specifications.

Particle Characteristics	Value
Nominal Power Plant Output	50 MW_e
Solar Multiple	2.0
Storage Capacity	6 hours
Power Block Cooling	Dry
Power Plant Location	Ouarzazate, Morocco
Annual Direct Normal Irradiation	2635 kWh/m^2yr
Design-Point Solar Irradiation	850 W/m^2
Design-Point Ambient Temperature	35°C

The DPS receiver has a nominal outlet temperature of 650°C, and is based on technology being developed in the Concentrated Solar Power in Particles (CSP2) project [9], described in an accompanying paper [10]. As such, power plants based on DPS technology are able to generate steam at temperatures up to 635°C, opening up the possibility of transitioning from subcritical to supercritical cycles. As can be seen in Fig. 3, the use of supercritical Rankine-cycles offers a significant efficiency improvement when compared to current state-of-the-art CSP plants.

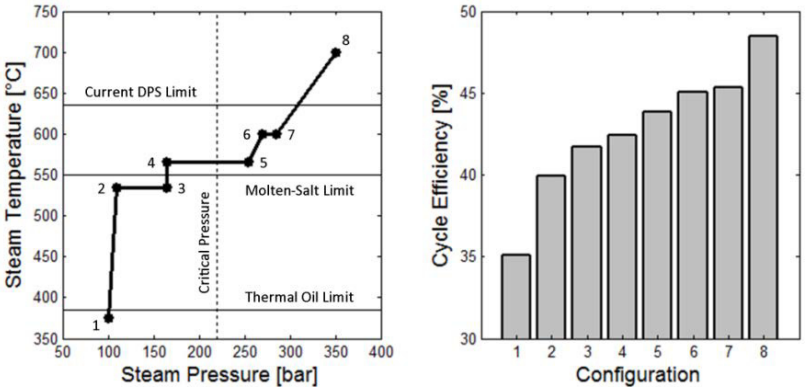

Fig. 3. Evolution of Standard Reheat Rankine-Cycle Configurations.
Cycle efficiencies assume an indirect dry-cooled condenser operating at 65°C and five-stage feedwater preheating.

Table 2. Operating Conditions of Typical Commercial Reheat Rankine-Cycle Configurations.

#	Power Cycle	Steam Conditions	
1	State-of-Art Parabolic Trough Plants	375°C	100 bar
2	State-of-Art Molten Salt Plants	535°C	115 bar
3	Old Subcritical Fossil Plants	535°C	165 bar
4	State-of-Art Subcritical Fossil Plants	565°C	165 bar
5	Old Supercritical Fossil Plants	565°C	255 bar
6	State-of-Art Supercritical Fossil Plants	600/610°C	270 bar
7	Advanced Supercritical Fossil Plants	600/620°C	285 bar
8	Ultra-Supercritical Fossil Plants	700/720°C	350 bar

Current supercritical Rankine cycles are designed for large power outputs in the region of 800 MW_e [11], and will need to be scaled-down for applications in CSP plants. The high-pressure steam-turbine units will be particularly

critical and may need to be redesigned in order to cope with the low volumetric flow rates and the resulting small blade sizes [13]. Radial turbines can be considered for the high pressure stages as they allow smaller flow areas, while the higher tip speeds permit more power to be extracted by each turbine stage. In general, radial turbines are well suited to applications with high pressures and low flow rates. Another approach is to operate the high pressure turbine at higher speeds and either couple the unit to the generator through a gearbox or incorporate high speed electrical switching circuitry [14]. Furthermore, in order to facilitate the deployment of concentrating CSP plants in arid locations where the solar insolation is strongest, the power block must be dry cooled. As such, an indirect (HELLER-type [15]) dry cooling system has been considered for all configurations.

4. Technical evaluation of the dense particle suspension power plant

The design and technical performance of the novel CSP plant will now be evaluated. Based on the power plant specifications given in Table 1, the power cycle is first calculated and the required heat exchanger network is established; the nominal mass flow of HTF can then be determined. Using the nominal HTF flow rate to the power block, as well as the temperatures at the inlet and outlet of the heat exchanger network, the receiver and storage units can be sized. Once the thermal efficiency and power demand of the receiver is fixed, a heliostat field is designed supply to the required thermal power to the receiver.

4.1. Reference molten-salt power plant

The performance of the DPS power plant is compared against a scaled-up version of a contemporary European molten salt CSP plant [16], re-designed using the reference parameters shown in Table 1. This power plant employs a conventional nitrate-salt receiver with a nominal outlet temperature of 565°C.

4.2. Power generation cycle and heat exchanger network

The power generation cycles for the DPS and molten salt CSP plants are designed based on the standard Rankine cycle configurations shown in Table 2. Configuration 7 is chosen for the DPS power plant in order to make best use of the high temperature HTF; the molten-salt power plant is based on configuration 2. The temperature-entropy diagrams for the resulting power cycles are shown in Fig. 4 and Fig. 5, and the performance of the cycles are compared in Table 3. Both configurations use an indirect dry-cooled condenser and five-stage feedwater preheating. The supercritical Rankine cycle offers a 5.5%-point efficiency increase, which reduces the thermal power input by 13.3%. The steam flowrate is also reduced by 9.3% leading to an 18.8% reduction in condenser fan power.

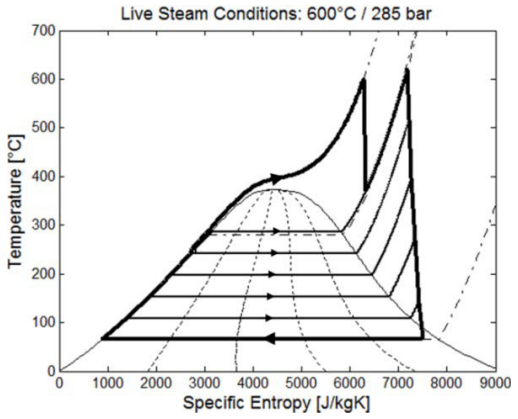

Fig. 4. Power cycle for particle suspension power plant.

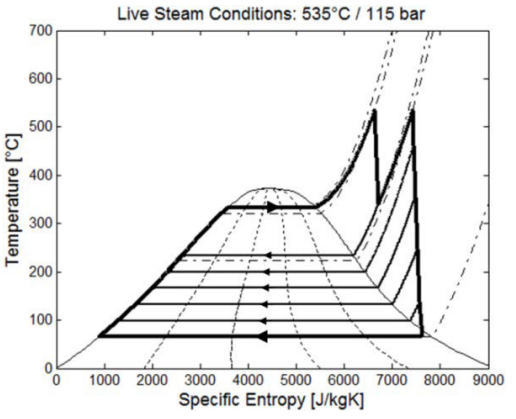

Fig. 5. Power cycle for molten salt power plant.

The temperature-enthalpy diagrams for the steam generator heat exchangers are shown in Fig. 6 and Fig. 7, and the reduced heat requirement of the supercritical Rankine-cycle can be clearly seen. The heat exchangers for the DPS system are based on the moving-bed solid particle heat exchanger concept [17]. The mass flow and terminal

temperatures of the HTF can also be determined, which is needed for the design of the receiver and storage units. The DPS power plant requires a total mass flow of 328 kg/s, with inlet and outlet temperatures of 650°C and 335°C, whereas the molten salt plant requires a total mass flow of 523 kg/s, with inlet and outlet temperatures of 565°C and 312°C. The temperature range for the DPS is thus 24.5% higher than for the molten salt plant.

Table 3. Performance of the power generation cycles.

Power Cycle Parameters	**Particle Suspension**	**Molten Salt**	
Live/Reheat Steam Pressure	285/65	115/25	[bar]
Live/Reheat Steam Temperature	600/620	535/535	[°C]
Live Steam Flowrate	43.1	47.5	[kg/s]
Gross Turbine Output	54.2	53.8	[MW]
Feedwater Pump Power	1.7	0.9	[MW]
Turbine Backpressure	25	25	[kPa]
Power Cycle Efficiency	45.4	39.9	[%]
Condenser Fan Power	1.40	1.75	[MW]
Net Power Block Efficiency	43.2	37.7	[%]

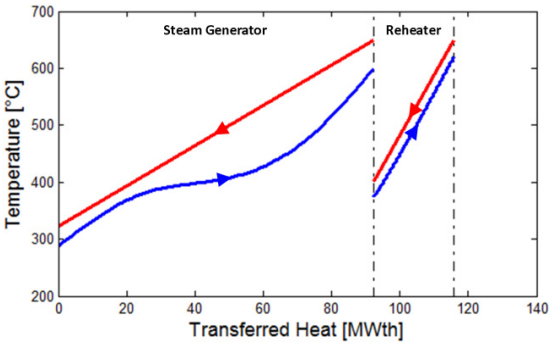

Fig. 6. Particle suspension steam generator.

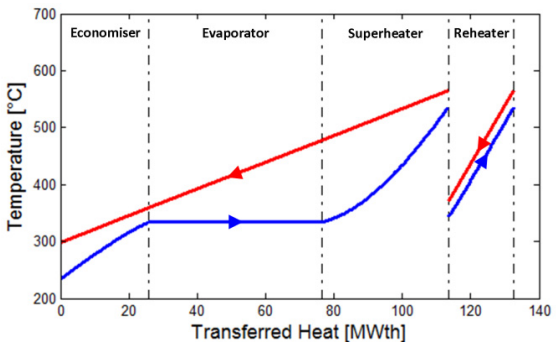

Fig. 7. Molten salt steam generator.

4.3. Receiver design and thermal efficiency

The design of the receiver for the DPS system is described in detail in an accompanying paper [10]; due to the larger thermal power requirement of the 50 MW_e CSP plant, a multi-unit receiver design is considered. The efficiency of the DPS receiver is 81.3%, compared to 86.0% for a typical molten salt receiver [18].

4.4. Storage density and tank sizing

Energy storage in the DPS power plant can be implemented through bulk storage of the solid particles. The specific heat of the particles is in the region of 1150 J/kgK with a density of 3210 kg/m^3, although this drops to a bulk density of 2054 kg/m^3 when accounting for the particle packing factor. This compares with a specific heat of 1560 J/kgK for the molten salt, with a density of 1680 kg/m^3. The increased temperature range of the DPS results in higher storage densities, with an energy density of 207 kWh_{th}/m^3 compared to 184 kWh_{th}/m^3, an increase of 12.5%.

The increase in storage density combined with the increased efficiency of the power cycle significantly reduces the storage volume. To guarantee 6 hours of full load storage, the DPS power plant requires two storage tanks, each with a volume of 3352 m^3, compared to two tanks of 4323 m^3 for the molten salt designs; this corresponds to a 22.5% reduction in the total volume of the storage tanks.

4.5. Heliostat field layout and efficiency

The heliostat fields for both configurations have been designed using WINDELSOL [19], which is based on the original DELSOL3 code from SANDIA National Labs [20]. The total power delivered by the heliostat field amounts to 284 MW for the DPS power plant and 308 MW for the molten salt configuration. The increased cycle efficiency of the DPS system is partly offset by the reduced receiver efficiency, as the power demand is only reduced by 7.8%. The heliostat field layouts for the two CSP plants are shown in Fig. 8 and Fig. 9.

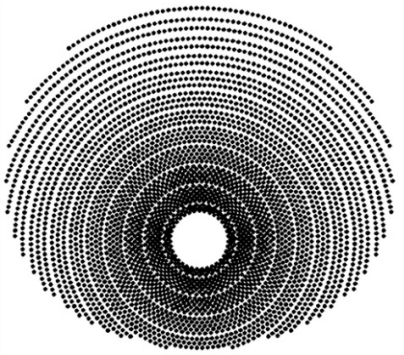

Fig. 8. Particle suspension heliostat field.

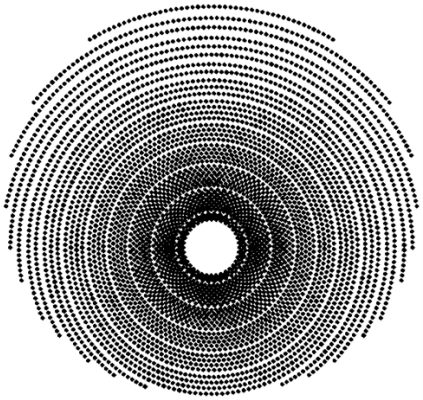

Fig. 9. Molten salt heliostat field.

The slight reduction in power requirement of the heliostat field for the DPS power plant results in a slight increase in the efficiency of the heliostat field, with an annual field efficiency of 61.0% for the DPS system compared with 59.7% for the molten salt power plant. In total, the heliostat field for the DPS power plant consists of 4184 heliostats, each with a surface area of 121 m^2, compared with 4629 for the molten salt system, a reduction of 9.6%, slightly more than the reduction in field output due to the increased efficiency.

4.6. Electricity yield and parasitic power plant loads

In both power plant configurations, parasitic electricity consumption is necessary to move the HTF between the receiver, storage and heat exchanger network. However, in the molten-salt power plant a significant amount of additional parasitic consumption occurs due to the need to prevent the salt freezing in the piping system; the parasitic consumption for heat tracing can amount to as much as 10% of the gross electrical output of the CSP plant [21]. As such, the use of the DPS as the HTF (which does not suffer from freezing problems) increases the net electricity yield and allows the cost per unit of output to be reduced.

Calculation of the parasitic consumption of the DPS receiver was covered in the accompanying paper [10]. With a tower height of 135 m (valid for both heliostat fields shown above) the nominal parasitic load for the DPS receiver amounts to 1.24 MW_e, with an additional 312 kW_e for the heat exchangers, equivalent to 3.1% of the nominal power plant output; the nominal parasitic load for the molten salt receiver is 1.63 MW_e. As such, the nominal parasitic loads for both systems are very similar, as the lower efficiency of the particle transport system compared to a simple liquid pumping system is offset by the lower mass flow that is required by the DPS system. However, the additional consumption for molten salt heat tracing needs to be calculated separately on an annual basis.

The electricity yield for the two power plants has been determined using in an in-house transient simulation tool, based on previous work by one of the authors [22]. This tool calculates the behavior of the CSP plant on an hourly basis, taking into account the off-design behavior of the power plant components. The calculated net output from the DPS power plant was 260 GWh_e/yr, compared to 242 GWh_e/yr for the molten salt plant, an increase of 7.4%; this difference is due almost entirely to the elimination of parasitic consumption for heat tracing.

5. Economic evaluation of the dense particle suspension power plant

The technical evaluation of the novel DPS power plant has revealed a number of favorable aspects, which act to improve the performance and electricity yield of the power plant. However, the higher operation temperature of the solar receiver and the increased pressure of the steam-cycle will also act to increase capital costs. In order to determine if the increased performance compensates for these costs, economic evaluation of the plant is required.

5.1. Power plant construction costs

Data on power plant equipment costs were sought for in the open literature and are shown in Table 4. Heliostat costs were taken from the reference power plant established by NREL [23], along with the solar receiver and storage costs for the molten salt configuration; power block costs for both configurations were taken from IEA data [24].

The solar receiver and storage for the DPS power plant are novel components for which established cost figures do not exist. The cost of the DPS receiver was estimated based on available data for a tubular air receiver [25], which operates in the same temperature range and with a similar heat transfer media; the resulting specific cost of the DPS receiver is 13% higher than the molten-salt receiver. The cost of the DPS storage was calculated from the cost of typical large-volume storage tanks and the cost of the particles themselves; a cost of 1.54 USD/kg was assumed for the silicon carbide particles [26], compared with 1.85 USD/kg for the nitrate salt [23]. Overall, the specific storage cost for the DPS system is 7.4% lower than for the molten salt system. Installation costs were assumed to be 15% of the capital costs [27] and the costs of engineering and procurement to be 5% of the installed cost [23]; contingency requirements were estimated as 10% of the installed cost [24].

Table 4. Power plant equipment costs.

Equipment Cost	**Particle Suspension**	**Molten Salt**	
Heliostat Field	200	200	[USD/m^2]
Receiver and Tower	195	173	[USD/kW_{th}]
Energy Storage	25	27	[USD/kWh_{th}]
Power Block	1675	1550	[USD/kW_e]

A breakdown and comparison of the construction costs for the power plants are shown in Table 5, and it can be seen that the high efficiency DPS power plant reduces the overall construction costs by 3.5%, as the increased cost of the power block is offset by reductions in the cost of the heliostat field and energy storage. Receiver costs are similar for both designs, as the higher specific cost of the DPS receiver is offset by the reduced thermal power requirement of the higher efficiency power block. The specific installed cost for the DPS and molten salt CSP plants are 5952 and 6166 USD/kW_e respectively, which are significantly below the typical value of 9810 USD/kW_e for a dry-cooled parabolic trough CSP plant [28]. Moving to higher-temperature CSP plants thus serves not only to increase the conversion efficiency but also to drive down the total installed cost per unit of capacity.

Table 5. Power plant construction costs.

Equipment Cost	**Particle Suspension**	**Molten Salt**		***Change***
Heliostat Field	101.3	112.0	[milUSD]	*- 9.6%*
Receiver and Tower	22.9	22.6	[milUSD]	*+ 1.3%*
Thermal Energy Storage	17.4	21.5	[milUSD]	*- 19.1%*
Power Block	83.8	77.5	[milUSD]	*+ 8.1%*
Equipment Installation	33.8	35.0	[milUSD]	*- 3.4%*
Engineering and Procurement	11.3	11.7	[milUSD]	*- 3.4%*
Contingencies	27.1	28.0	[milUSD]	*- 3.2%*
Total Construction Cost	297.6	308.3	[milUSD]	*- 3.5 %*

5.2. Levelised cost of electricity

In order to quantify the reduction in electricity costs that results from the increased yield and reduced cost of the DPS power plant, it necessary to determine the levelised cost of electricity (LCOE). This can be calculated using Equation (1), where C_0 is in the total overnight construction cost, $C_{O\&M}$ the annual operation and maintenance costs, C_{dec} the end-of-life decommissioning costs and E_{net} the net annual electricity yield (see §4.6).

$$\mathrm{LCOE} = \frac{\alpha \cdot C_0 + C_{O\&M} + \beta \cdot C_{dec}}{E_{net}} \tag{1}$$

The capital return factor α and the decommissioning accumulation factor β can be calculated using Equation (2), based on the real interest rate i, the plant operating lifetime n_{op} and the annual insurance rate k_{ins}. Standard values for these financing parameters can be obtained from the ECOSTAR report [25], giving α = 9.88% and β = 0.88%.

$$\alpha = \frac{i \cdot (1+i)^{n_{op}}}{(1+i)^{n_{op}} - 1} + k_{ins} \quad \text{and} \quad \beta = \frac{i}{(1+i)^{n_{op}} - 1} \tag{2}$$

The annual operation and maintenance costs can be calculated as a percentage of the initial capital costs, using an assumed attrition rate of 2%/yr for the power block and storage, 3%/yr for the heliostat field, due to a high rate of mirror breakage, and 4%/yr for the receiver due to the combination of innovative design and harsh operating conditions. Decommissioning costs can be assumed to be equal to 5% of the initial construction costs [24].

The final values of the LCOE for the two power plants are 141 USD/MWh$_e$ for the DPS configuration, compared to 158 USD/MWh$_e$ for the molten salt power plant, a reduction of 10.8%. The improved technical performance of the DPS power plant therefore leads to a significant reduction in the cost of electricity, despite the higher costs associated with the advanced receiver and power block technology.

6. Conclusions

A detailed techno-economic analysis has been performed for a 50 MW$_e$ CSP plant based on the use of a novel dense particle suspension as the heat fluid. The particle suspension can operate at higher temperatures than conventional molten-salt systems, allowing the use of a higher efficiency power block based on a supercritical Rankine-cycle. This boosts the thermal conversion efficiency from 37.7% (for a typical dry-cooled molten-salt power plant) to 43.2%, an increase of 5.5%-points.

The increased cycle efficiency leads to a reduction in thermal power requirements, which reduces the size of the heliostat field by 9.6% and, combined with the increased temperature range available to the particle suspension, increases the energy density of the storage units by 12.5%, relative to the reference molten salt plant. Parasitic power consumption was also significantly reduced due to the elimination of the need for heat tracing. The combination of these technological changes allowed the installed cost of the novel power plant to be reduced by 3.5%, from 6166 to 5952 USD/kW$_e$, while the electricity yield was increased by 8.2%. The resulting levelised cost of electricity was in the region of 141 USD/MWh$_e$, a reduction of 10.8% compared to the reference molten salt power plant.

The study clearly demonstrated the importance of combining technical performance calculations with economic analysis and cost predictions, as the reduced size and costs of the heliostat field and storage units were partially offset by increases in the cost of the solar receiver and power block. It is necessary to carefully weigh the effects of the different performance and cost changes in order to determine the overall impact on the cost of electricity.

The results have shown the potential for new, high temperature heat transfer fluids to improve the performance and cost effectiveness of CSP technology. The dense particle suspension is a promising option, allowing the use of more efficient power conversion cycles and facilitating energy storage, which serves to reduce the cost of electricity. In this study a receiver temperature limit of 650°C was considered; future developments in the CSP2 project will

likely increase this temperature to 750°C, allowing further performance improvements and opening the possibility to use advanced power generation cycles (such as supercritical CO_2 cycles).

The results presented here considered only a single power plant configuration (a solar multiple of 2 and 6 hours of storage). However, as the results showed significant reductions in the cost of storage (19.1%) and well as the solar collector (9.6%) it likely that larger storage units and heliostat fields will be economically viable. Larger storage capacities and solar multiples will increase the capacity factor of the power plant and improve the utilization of the more expensive supercritical power block. Optimization of the new particle suspension power plant will form the basis of a follow-up study, seeking further reductions in the cost of electricity.

Acknowledgements

This work has been co-funded by the European Commission as part of the Concentrated Solar Power in Particles project (CSP2, FP7 project number: 282932), the support of which is gratefully acknowledged. Additional thanks are given to our partners in the CSP2 project for their valuable feedback and advice on this work.

References

[1] International Energy Agency, 2011, *Renewable Energy Technologies: Solar Energy Perspectives*, OECD/IEA Publications, Paris
[2] J. Sawin, R. Adib, J. Skeen et al., 2013, *Renewables 2013 - Global Status Report*, Renewable Energy Policy Network, United Nations Environment Programme, Paris
[3] A. Fernández-García, E. Zarza, L. Valenzuela et al., *Parabolic-Trough Solar Collectors and their Applications*, Renewable and Sustainable Energy Reviews, Volume 14/7 (2010), pp. 1695 – 721
[4] M. Romero, J. González-Aguilar, *Solar Thermal CSP Technology*, WIREs Energy and Environment, Volume 3 (2014), pp. 42 – 59
[5] D. Geldart, 1973, *Types of Gas Fluidization*, Power Technology, Volume 7, pp. 285 – 92
[6] G. Flamant, D. Gauthier, H. Benoit et al., *A New Heat Transfer Fluid for Concentrating Solar Systems: Particle Flow in Tubes*, SolarPACES Conference, Energy Procedia, Volume 49 (2014), pp. 617 – 26
[7] G. Flamant, D. Gauthier, H. Benoit et al., *Dense Suspension of Solid Particles as a New Heat Transfer Fluid for Concentrated Solar Thermal Plants: On-Sun Proof of Concept*, Chemical Engineering Science, Volume 102 (2013), pp. 567–76
[8] P. Falcone, J. Noring, J. Hruby, 1985, *Assessment of a Solid Particle receiver for a High Temperature Solar Central Receiver System*, SANDIA National Laboratories (SAND85-8208)
[9] Concentrated Solar Power in Particles: http://www.csp2-project.eu/
[10] A. Gallo, J. Spelling, M. Romero et al., 2014, *Preliminary Design and Performance Analysis of a Multi-Megawatt Scale Dense Particle Suspension Receiver*, Proceedings of the International SolarPACES Conference, September 16 – 20, Beijing
[11] F. Cziesla, H. Kremer, U. Much et al., 2009, *Advanced 800+ MW Steam Power Plants and Future CCS Options, Siemens Energy Sector*, Proceedings of COAL-GEN Europe, September 1 – 4, Katowice
[12] Siemens Industrial Turbomachinery, 2010, *Steam Turbines for CSP Plants*, Siemens Energy Sector, Erlangen
[13] A. Bölcs, 2001, *Turbomachines Thermiques*, Volume I, Ecole Polytechnique Fédérale, Lausanne
[14] C. Singer, R. Buck, R. Pitz-Paal et al., *Assessment of Solar Power Tower Driven Ultrasupercritical Steam Cycles Applying Tubular Central Receivers with Varied Heat Transfer Media*, Journal of Solar Energy Engineering, Volume 132 (2010)
[15] A. Conradie, D. Kröger, *Performance Evaluation of Dry-Cooling Systems for Power Plant Applications*, Applied Thermal Engineering, Volume 16 (1996), pp. 219 – 32
[16] J. Burgaleta, S. Arias, D. Ramírez, 2012, *Gemasolar: The First Tower Thermosolar Commercial Plant with Molten Salt Storage*, Proceedings of the International SolarPACES Conference, September 11 – 14, Marrakech
[17] T. Baumann, S. Zunft, 2012, *Moving Bed Heat Exchanger for Solar Central Receiver Power Plants: A Multi-Phase Model and Parameter Variations*, Proceedings of the International SolarPACES Conference, September 11 – 14, Marrakech
[18] J. Ortega, J. Burgaleta, F. Téllez, *Central Receiver System Solar Power Plant Using Molten Salt as Heat Transfer Fluid*, Journal of Solar Energy Engineering, Volume 130 (2008)
[19] AICIA-CIEMAT-SOLUCAR, 2002, *WINDELSOL 1.0 Users Guide*
[20] B. Kistler, 1986, *A User's Manual for DELSOL3,* SANDIA National Laboratories (SAND86-8018)
[21] J. Pacheco, 2002, *Final Test and Evaluation Results from the Solar Two Project*, SANDIA National Laboratories (SAND2002-0120)
[22] J. Spelling, B. Laumert, 2014, *Thermoeconomic Evaluation of Solar Thermal and Photovoltaic Hybridization Options for Combined-Cycle Power Plants*, GT 2014- 25173, Proceedings of the ASME Turbo Expo, June 16 – 20, Düsseldorf
[23] C. Turchi, G. Heath, 2013, *Molten Salt Power Tower Cost Model for the System Advisor Model*, National Renewable Energy Laboratory, (NREL/TP-5500-57625)
[24] International Energy Agency, 2010, *Projected Cost of Generating electricity*, OECD/IEA Publications, Paris
[25] R. Pitz-Paal, J. Dersch, B. Milow et al. (editors), 2004, *ECOSTAR: European Concentrated Solar Thermal Road-Mapping*

[26] Shandong Jinmeng New Material Co., Ltd., 2014, *Corporate Communication*
[27] M. Peters, K. Timmerhaus, 1991, *Plant Design and Economics for Chemical Engineers*, Fourth Edition, McGraw-Hill, New York
[28] C. Turchi, 2010, *Parabolic Trough Reference Plant for Cost Modeling with the Solar Advisor Model*, National Renewable Energy Laboratory (NREL/TP-550-47605)